*J. Fluid Mech.* (2010), *vol.* 652, *pp.* 65–73.  
doi:10.1017/S0022112010001497

# Scaling of global properties of turbulence and skin friction in pipe and channel flows

VICTOR YAKHOT[1], SEAN C. C. BAILEY[2] AND ALEXANDER J. SMITS[3]†

[1]Department of Aerospace and Mechanical Engineering, Boston University, Boston, MA 02215, USA

[2]Department of Mechanical Engineering, University of Kentucky, Lexington, KY 40506, USA

[3]Department of Mechanical and Aerospace Engineering, Princeton University, Princeton, NJ 08544, USA

(Received 12 January 2010; revised 18 March 2010; accepted 18 March 2010)

Experimental data on the Reynolds number dependence of the area-averaged turbulent kinetic energy $K$ and dissipation rate $\mathscr{E}$ are presented. It is shown that while in the interval $Re_D > 10^5$ the total kinetic energy scales with friction velocity ($K/u_*^2 = \text{const}$), a new scaling law $K/\langle U\rangle^2 \propto K/(u_*^2 Re_D^\theta) = \text{const}$ ($\theta \approx 1/4$) has been discovered in the interval $Re_D < 10^5$. It is argued that this transition is responsible for the well-known change in the scaling behaviour of the friction factor observed in pipe and channels flows at $Re_D \approx 10^5$.

## 1. Introduction

Experimental studies of the friction factor $\lambda$ in turbulent pipe and channel flows have revealed two distinct intervals: $\lambda \propto Re_D^{-1/4}$ proposed by Blasius for $Re_D < 10^5$ and $\lambda \propto Re_D^{-\theta}$ for $Re_D > 10^5$ Schlichting (1968). For a pipe, $\lambda = 8\tau_w/\rho\langle U\rangle^2 \equiv 8u_*^2/\langle U\rangle^2$, where $\tau_w$ is the wall friction, $Re_D = \langle U\rangle D/\nu$, $\langle U\rangle$ is the area-averaged or bulk velocity, $D$ is the pipe diameter ($=2R$), and $\rho$ and $\nu$ are the fluid density and kinematic viscosity, respectively. Today's consensus on the high-Reynolds-number asymptotics has $\theta \to 0$ so that

$$\frac{1}{\sqrt{\lambda}} \propto \ln Re_D. \tag{1.1}$$

As to the lower-Reynolds-number Blasius scaling, it has been regarded mostly as a convenient empirical curve fit (Nagib, Chauhan & Monkiewitz 2007). Recently, however, this scaling has been derived from an interesting model based on assumed coherent structures and Kolmogorov energy spectrum in the sublayer (Gioia & Chakraborty 2006). One problem with this approach is that it gives the Blasius scaling for all turbulent flow Reynolds numbers, which contradicts the experimental data. Another problem is that Kolmogorov's spectrum, or indeed any other algebraically decreasing energy spectrum, has not been observed in the sublayer, and it is well established that the dynamics of turbulence production in the sublayer are intermittency-dominated (Lee, Yeo & Choi 2004). Here we take a different approach and examine the proposition that the change in scaling reflects a transition from one state of turbulence to another.

† Email address for correspondence: asmits@princeton.edu

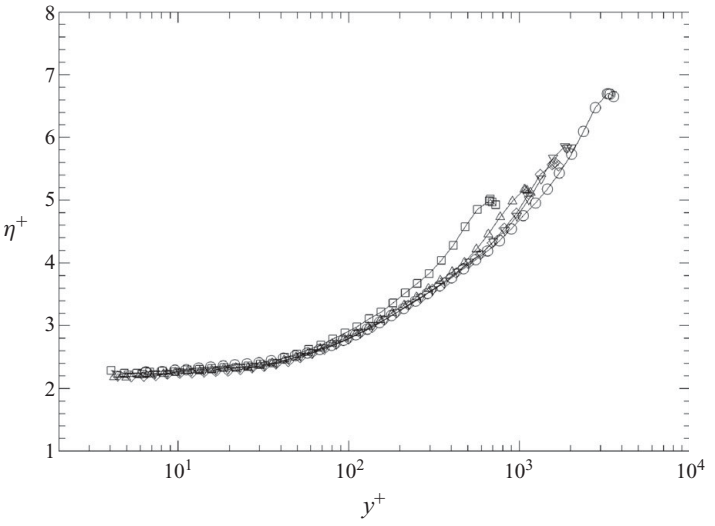


FIGURE 1. Distribution of the dissipation scale in a fully developed turbulent pipe flow. □, $Re_D = 25 \times 10^3$; △, $45 \times 10^3$; ◇, $65 \times 10^3$; ▽, $80 \times 10^3$; ○, $150 \times 10^3$.

We expect that the magnitude of a scaling exponent reflects the basic physical mechanisms and symmetries of a problem, and therefore the transition from one scaling exponent to another is often accompanied by changes in the basic properties of a system. A good example is given by the transition from 'soft' to 'hard' turbulence in a convection cell. It has been shown that above a critical Rayleigh number, a new production mechanism emerges: the turbulence is generated by thermal plumes emitted by unstable boundary layers into the bulk of a Bénard convection cell. This effect is responsible for the change observed in the scaling exponent $\alpha$ in the Nusselt–Rayleigh number relationship $Nu \propto Ra^{\alpha}$.

In this paper, searching for a transition from one state of turbulence to another, we first examine the Reynolds number dependence of global turbulence characteristics such as $K$, the streamwise component of the mean turbulent kinetic energy $\overline{u'^2}/2$ averaged over the cross-sectional area of the pipe. That is,

$$K = \frac{1}{\pi R^2} \int_0^R \left( \frac{1}{2} \overline{u'^2} \right) 2\pi r \, \mathrm{d}r, \tag{1.2}$$

where $r = R - y$, and $y$ is the wall-normal distance. In our notation, $u'$, $v'$, and $w'$ are the streamwise, wall-normal and spanwise velocity fluctuations, respectively. We will demonstrate by experiment and analysis that (i) in the high-Reynolds-number regime where $Re_D > 10^5$, $K \propto u_*^2$, and (ii) in the Blasius regime where $Re_D \leqslant 10^5$, $K \propto \langle U \rangle^2$ and $K/(u_*^2 Re^{1/4}) \approx$ constant. It is then argued that this transition is responsible for the Blasius scaling behaviour of skin friction observed in pipe and channel flows for $Re_D \leqslant 10^5$.

## 2. Experimental results

The behaviour of the dissipation scale $\eta^+ = \eta u_*/\nu$ for pipe flow Reynolds numbers in the range $25 \times 10^3 \leqslant Re_D \leqslant 150 \times 10^3$ is shown in figure 1, where $y^+ = y u_*/\nu$. The dissipation rate was calculated by integrating the dissipation spectrum that was estimated from the streamwise power spectrum using the one-dimensional

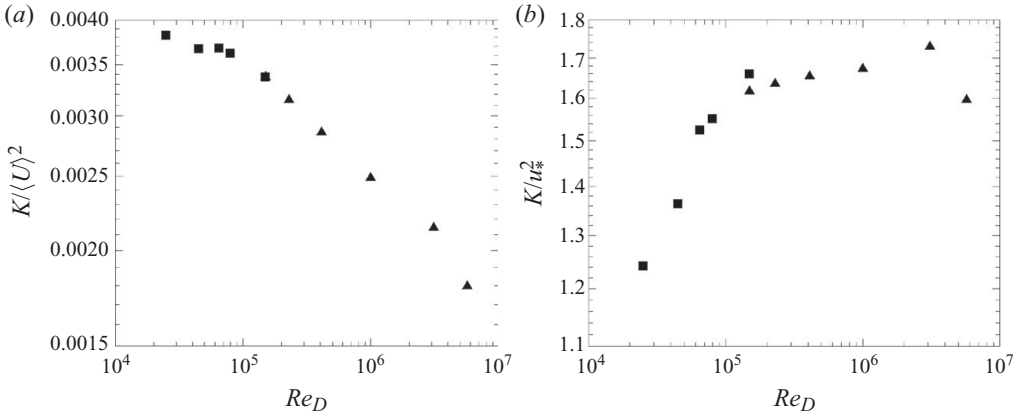


FIGURE 2. Reynolds number dependence of the normalized kinetic energy $K$. ■, Hultmark *et al.* (2010); ▲, Morrison *et al.* (2004). Data shown as $K/\langle U\rangle^2$ (*a*) and as $K/u_*^2$ (*b*).

approximation, as described by Bailey *et al.* (2009). For details of the experiment, see Hultmark, Bailey & Smits (2010). We see that within the sublayer where $0 < y^+ < y_s^+ \approx 50$, $\eta^+(y) = \text{const}$ ($\approx 2$), independent of $y^+$ and $Re_D$, and so

$$\mathscr{E} \propto \frac{u_*^4}{\nu}. \tag{2.1}$$

This result is consistent with the expression for the locally fluctuating dissipation scale $\mathscr{E} \approx (\delta_\eta u)^4/\nu$ derived and tested in numerical experiments on low-Reynolds-number flows by Schumacher, Sreenivasan & Yakhot (2007), if $\delta_\eta u \equiv (u(x+\eta) - u(x))_{rms} = u_*$. Also in the sublayer ($y \leqslant y_s$),

$$\frac{\eta}{D} = \frac{\eta^+}{2R_*} \approx \frac{\text{const}}{R_*},$$

where $R_* = Ru_*/\nu$. Because this result is independent of $y$, it is valid at $y = y_s$. Furthermore, because the width of the sublayer is proportional to the viscous scale $\nu/u_*$, and therefore proportional to the dissipation scale $\eta$, we have

$$\eta(y) \propto y_s \propto DR_*^{-1}. \tag{2.2}$$

This result differs from the classic Kolmogorov estimate $\eta \propto DRe^{-3/4}$ proposed for homogeneous and isotropic turbulence. Interestingly, for a given Reynolds number, the local value of the dissipation scale in the sublayer depends on the diameter of the pipe, a global property. It will become clear that this non-trivial feature is related to the coherent motions controlling turbulence production. For the Reynolds numbers shown in figure 1 ($R_* = 700$, 1100, 1500, 1900, 3300), $\eta(y^+)$ collapses onto a single curve for $y^+ < 200$, 500, 700, 900, 1400, respectively, that is, the curves collapse in the region $y/R < 0.5$ for $Re_D > 25 \times 10^3$, which points to universality of the dimensionless function $\mathscr{E}^+ = \mathscr{E}\nu/u_*^4$.

In figure 2, the area-averaged mean kinetic energy $K$ defined by (1.2), normalized by $\langle U\rangle$ and $u_*$, is shown as a function of Reynolds number. All measurements were taken in the Princeton Superpipe described by Zagarola & Smits (1998). The data for $Re_D \leqslant 150 \times 10^3$ are taken from Hultmark *et al.* (2010), and the higher-Reynolds-number data were taken from Morrison *et al.* (2004). Note that the high-Reynolds-number data of Morrison *et al.* (2004) could be subject to filtering effects due to

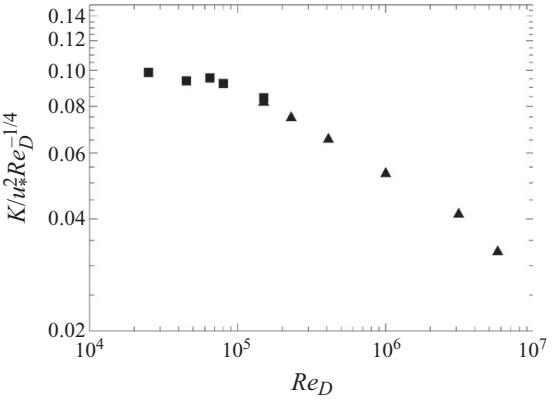


FIGURE 3. The scaled mean kinetic energy $K/u_*^2 Re_D^{1/4}$ as a function of Reynolds number. ■, Hultmark *et al.* (2010); ▲, Morrison *et al.* (2004).

inadequate spatial resolution of the measurement probe. However, as observed by Hutchins *et al.* (2009), this filtering effect has the greatest impact near the wall where the length scales of the turbulence are small, and reduces further from the wall. Thus, these effects have little impact on the integrated statistics. For example, this filtering will be worst at the highest Reynolds number of Morrison *et al.* (2004), but at this Reynolds number, the region below $y^+ < 1000$, where such filtering effects are expected to be important, represents only 2 % of the total integral.

In figure 2, a previously unreported transition at $Re_D \approx 10^5$ from $K \propto \langle U \rangle^2$ to $K \propto u_*^2$ is clearly seen. To obtain the scaling exponent $\theta$, in figure 3 we show that $K/(u_*^2 Re^{1/4}) \approx$ const in the low-Reynolds-number interval. Together with $K \propto \langle U \rangle^2$, it follows that in the range $Re_D < 10^5$,

$$\lambda = \frac{8u_*^2}{\langle U \rangle^2} \propto \frac{u_*^2}{K} \propto Re_D^{\theta} \tag{2.3}$$

with $\theta \approx -1/4$, as in the classical Blasius fit.

In figure 4, we show the compilation of experimental data on $K_v$ and $K_k$ as a function of $Re_D$, where $K_v$ is the wall-normal component of the mean turbulent kinetic energy $\overline{v'^2}/2$ averaged over the cross-sectional area of the pipe, and $K_k$ is the turbulent kinetic energy $(\overline{u'^2} + \overline{v'^2} + \overline{w'^2})/2$ averaged over the cross-sectional area of the pipe, both defined in a manner similar to $K$; see (1.2). The wall-normal and azimuthal turbulence components, $\overline{v'^2}$ and $\overline{w'^2}$, are difficult to measure accurately at high Reynolds number. As such, both components were unavailable from the Hultmark *et al.* (2010) and Morrison *et al.* (2004) data sets, and the azimuthal component was unavailable from the Zhao & Smits (2007) data set. The magnitudes of the missing components were therefore estimated by examining the scaling of $\overline{v'^2}/\overline{u'^2}$ and $\overline{w'^2}/\overline{u'^2}$ in the data sets where these velocity components were available. It was found that these ratios follow an inner scaling up to $y^+ < 100$, and then increase linearly from the value at $y^+ = 100$ to a nearly isotropic value at $y/R = 1$, allowing a reasonable estimate of $\overline{v'^2}$ and $\overline{w'^2}$ from the known values of $\overline{u'^2}$.

As seen in figure 4, while $K_v$ (and also $K_w$, not shown here) scale with $\langle U \rangle^2$ over the entire range $4000 \leqslant Re_D \leqslant 10^5$, $K_k$ only shows this dependence over a somewhat narrower interval $15\,000 \leqslant Re_D \leqslant 10^5$. There also appears to be an influence of transition. The Princeton Superpipe flow features a relatively high transitional

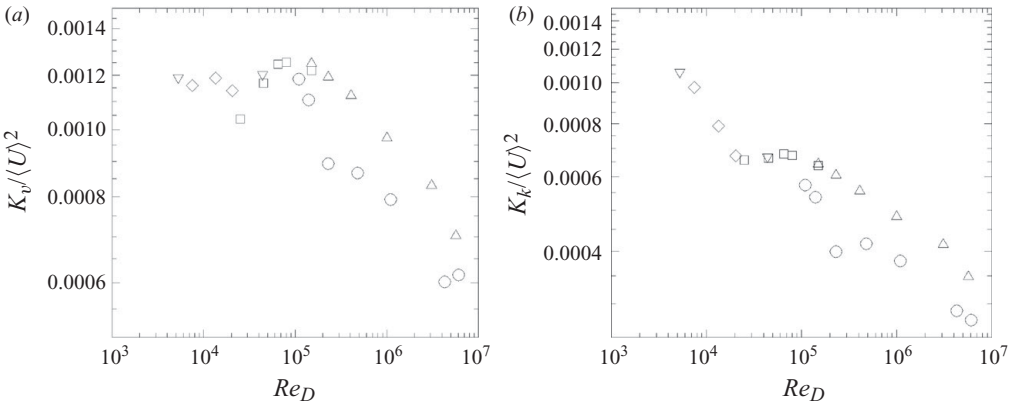


FIGURE 4. The scaled area-averaged variance $K_v$ ($a$) and $K_k$ ($b$) as a function of Reynolds number. □, current data set; △, Morrison *et al.* (2004); ◇, Durst, Jovanovic & Sender (1995); ▽, Wu & Moin (2008); ○, Zhao & Smits (2007).

Reynolds number, with $Re_{D,tr} \approx 10^4$, compared to the value of 2300–3000 typically observed in physical and numerical experiments. If we adopt $Re_D - Re_{D,tr}$ as the most appropriate Reynolds number, then the Superpipe data would be expected to shift to the left, relevant to the other data. Hence, in the vicinity of transitional Reynolds number, the streamwise component $u'$, which is dynamically 'passive' in that it does not contribute significantly to the mixing and turbulence production processes, dominates the scaling behaviour of total kinetic energy. This feature stresses the importance of the $y$- and $z$-components of the velocity field in the transition observed in the friction factor at $Re_D \approx 10^5$. Given these differences, we may expect universality in pipe and channel flows only in the interval $Re_D \geqslant 10^4$.

## 3. Analysis of Blasius scaling

Here we are interested in proposing a theory for the low-Reynolds-number range $Re_D < 10^5$ where we find $K/\langle U\rangle^2 = \text{const}$. Schumacher *et al.* (2007) showed that even at relatively low Reynolds numbers ($R_\lambda \geqslant 20$) the moments of the velocity derivatives are characterized by anomalous exponents identical to those observed in high-Reynolds-number flows ($R_\lambda \to \infty$). In other words, the smallest-scale dynamics of a flow with $R_\lambda \geqslant 20$ are identical to that of a flow at $R_\lambda \to \infty$. In addition, Bailey *et al.* (2009) investigated small-scale properties of turbulence in a fully developed pipe flow in the Princeton Superpipe. Remarkably, the results obtained in the strongly anisotropic logarithmic region (at $y/R \approx 0.1$) were identical to those obtained at the centerline of the pipe where the flow is close to isotropic. Moreover, the results agreed extremely well with well-resolved numerical simulations of isotropic and homogeneous turbulence by Schumacher (2007) and Schumacher *et al.* (2007) and theoretical predictions by Yakhot (2006). We infer that all conclusions of statistical theory of intermittent turbulence, valid in the limit $Re \to \infty$, can be used to describe anomalous exponents of the moments of velocity derivatives in relatively low-Reynolds-number flows, including wall flows, even where there is no evidence for the presence of an inertial range. Hence, the inertial range is passive, its extent is unimportant, and the only relevant large-scale parameter is the magnitude of the energy flux. If this is so, then

the large-scale structures, isotropic or not, merely produce the flux of kinetic energy dissipated at the close-to-isotropic dissipation scales.

We now apply these concepts to a fully developed turbulent channel flow of height $2h$ driven by a pressure gradient $\partial p/\partial x$, where $x$ is the streamwise direction and $y$ is the wall-normal direction measured from one wall. The Navier–Stokes equation for a constant property fluid reduces to

$$\frac{\mathrm{d}p}{\mathrm{d}x} = \frac{\mathrm{d}}{\mathrm{d}y}\left(\tau_{xy} + \mu\frac{\mathrm{d}U}{\mathrm{d}y}\right), \tag{3.1}$$

where $\tau_{xy} = -\rho\overline{u_x u_y}$ is the Reynolds stress. By integrating over the interval $0 \leqslant y \leqslant h$ we find the stress at the wall:

$$\tau_w = \mu\left.\frac{\partial U}{\partial y}\right|_0 = h\frac{\mathrm{d}p}{\mathrm{d}x} = \rho u_*^2.$$

A similar expression with $R/2$ instead of $h$ is easily derived for the pipe flow. To obtain the mean stress balance in the sublayer, we integrate (3.1) over the interval $0 \leqslant y \leqslant y_s$. Hence,

$$\frac{y_s}{h} + \frac{\tau_{xy}}{\tau_w} = 1 - \frac{\mu}{\tau_w}\left.\frac{\partial U}{\partial y}\right|_s. \tag{3.2}$$

Assuming (this will be tested below) that at the edge of sublayer where $y = y_s$, the viscous stress is negligibly small compared with the wall stress, and taking $y_s \ll h$, we obtain

$$\tau_{xy}(y_s) \approx \tau_w = \rho u_*^2. \tag{3.3}$$

Relation (3.3) is in quantitative agreement with results of numerical simulations of a very low-Reynolds-number channel flow ($h^+ = 180$) by Boeck *et al.* (2010), who found $\tau_{xy}(y_s)/\tau_w \approx 0.75$ at $y = y_s$. The value slowly increases with Reynolds number so that at $h^+ = 2000$ the value exceeds 0.9 (Hoyas & Jiménez 2005, 2006). Hence, the stress at the wall is approximately equal to the Reynolds stress at the edge of the sublayer $y = y_s$, where we can apply our knowledge of statistical turbulence theory.

Wall-bounded turbulence is often described in terms of a two-layer model, with a region near the wall where viscosity is important, and an outer region where it is not. We perceive the sublayer as a relatively slow, strongly intermittent flow, where the turbulence is characterized by small-scale phenomena such as dissipation and enstrophy, which are concentrated in close proximity to the wall. We also know that in this region the turbulence production is approximately twice as large as the dissipation rate (Kim, Moin & Moser 1987), with the balance released to the core by the turbulent diffusion mechanism. The sublayer is dominated by thin ($O(\eta)$) and long ($O(h)$), unstable structures (low-speed streaks). It is well documented that the formation of hair-pin vortices and their violent breakdown are responsible for turbulence generation in the core. The $O(h)$ length of these vortices is responsible for the appearance of the global length $h$ (equivalently, $R$ or $D$) in (2.2) describing the local dissipation scale $\eta$.

The turbulent velocity fluctuations in the near-wall region scale closely with $u_*$. In pipe flows, this variation appears to be universal (Hultmark *et al.* 2010), while in boundary layers and channels there is a slow variation with Reynolds number, indicating a weak influence of the outer layer structures on the inner layer behaviour. The breakdown of the streaks (bursts), emitted with a wall-normal component of velocity $\approx u_*$, reaches the proximity of the centerline $y \approx h$ with a time delay $T \approx h/u_*$,

treated here as an interaction time. This process resembles turbulence generation by the plumes in a Bénard convection cell.

In the low-Reynolds-number range considered here, we assume that the interaction between well-separated bursting structures can be neglected. It is this localization that is the main cause of strong intermittency of turbulence production (Lee *et al.* 2004). The momentum exchange for an individual burst is $2\rho\Omega(\langle U\rangle - au_*)$, where $\Omega$ is the mean volume of a single bursting structure, and $au_*$ is the characteristic $x$-component of its velocity. Thus, defining the mean total number $N$ of these structures and using the estimated interaction time, the total stress acting on an interface of area $S$ at $y \approx y_s$ is

$$\tau_{xy}(y_s) \approx \frac{2N\rho\Omega(\langle U\rangle - au_*)u_*}{Sh} \approx \rho u_*^2. \tag{3.4}$$

Because $2Sh = V$ is the entire volume, we define $\gamma \equiv N\Omega/V$ as the volume fraction of the flow occupied by the dissipating (bursting) structures. The parameter $\gamma$ can be understood as a conditional probability of a dissipation structure (dissipation scale) formed as a result of an intermittent instability of a sublayer. A possible interpretation is that both the integral and the dissipation scales in wall flows are simultaneously formed by this instability, and then fill the bulk flow with turbulent velocity fluctuations. In the low-Reynolds-number flows we are interested in here, a limited range of intermediate scales can be generated in the core as a result of a convolution or secondary instability of the emitted thin and long structures. We would like to stress that, because according to our data (see figure 1 and expression (2.2)), the thickness of sublayer is $y_s = O(1/R_*)$, no scale smaller than $y_s$ can be generated in the outer region of the flow.

To assess the magnitude of the constant $a$, we note that $\tau_{xy}(y_s) = -\rho\overline{u'v'} \approx \rho u'_{rms} v'_{rms}\gamma$, where $\gamma$ is the conditional probability (dimensionless) of the bursting events. Taking into account that, according to our experimental data, $u'_{rms} \propto \langle U\rangle$ (with $u'_{rms}/\langle U\rangle \ll 1$), and comparing this estimate with expression (3.4), we conclude that $au_*/\langle U\rangle \ll 1$. Hence,

$$\gamma\langle U\rangle \propto u_* \propto \sqrt{\lambda}\langle U\rangle. \tag{3.5}$$

The parameter $\gamma$ can be found from the theory of intermittency (for example, see Frisch 1995). It has been shown that

$$Re^{-d_2}\overline{\mathscr{E}^2} \approx \left(\frac{\eta}{L}\right)^{\mu}\overline{\mathscr{E}^2} \approx \overline{\mathscr{E}}^2, \tag{3.6}$$

with anomalous dimension $d_2 \approx 0.157$. Numerical simulations of low-Reynolds-number isotropic turbulence gave $d_2 \approx 0.152$ (Schumacher *et al.* 2007). The ratio $\gamma \approx (\eta/L)^{\mu}$ is exactly the parameter we are looking for. In relation (3.6), derived for isotropic turbulence, the Reynolds number is $Re = u^0_{rms}L/\nu$, where $L$ is the integral length scale. In the case of a sublayer, $u^0_{rms} = v_{rms} \approx u_*$ and the integral scale $L = h$, so that in relation (3.6) $Re = R_*$ and, as we saw earlier $\eta \propto 1/R_*$, giving $\mu = d_2$. Thus,

$$\gamma \propto \left(\frac{\eta}{h}\right)^{d_2} \propto R_*^{-d_2}. \tag{3.7}$$

Taking into account that $\sqrt{\lambda} \propto u_*/\overline{U} \approx R_*/Re_h$, we obtain

$$\lambda \propto \gamma^2 \propto R_*^{-2d_2} \tag{3.8}$$

and, because

$$\lambda \approx R_*^{-2d_2} \approx \left(\frac{R_*}{Re_h}\right)^2,$$

we find that the two Reynolds numbers are related according to $Re_h \approx Re_*^{1+d_2}$, so that

$$\lambda \propto Re_h^{-\theta} \tag{3.9}$$

with $\theta = 2d_2/(1+d_2)$. Hence, $\theta \approx 0.27$ and 0.26 for $d_2 = 0.157$ and $d_2 = 0.152$ (the values given by Schumacher *et al.* 2007), respectively, which are very close to the Blasius value $\theta = 1/4$. An entirely similar result can be obtained for pipe flow.

We can also estimate the Reynolds number range over which our model may be valid. It was assumed that the emitted structures reach the proximity of the centerline relatively undistorted on the time scale $T \approx h/u_*$. On the way, these thin and long entities will be dissipated by diffusion on a time scale $T_d \approx y_s^2/\nu$, so that they can reach the centerline only if $T < T_d$, or

$$\frac{h}{u_*} < \frac{y_s^2}{\nu},$$

so that

$$R_* < (y_s^+)^2. \tag{3.10}$$

For $y_s^+ \approx 20-50$, this gives the upper bound for the validity of the scaling arguments considered here as $R_* < 400$–$2500$, which corresponds well with the range of Blasius scaling seen in experiments.

We would like to stress that the model developed here is based entirely on a detailed consideration of the dissipative structures in a manner described by Schumacher *et al.* (2007). No assumptions regarding the spectra were necessary.

The Office of Naval Research (ONR) is gratefully acknowledged for their financial support under grant N00014-09-1-0263 (Dr Ron Joslin).

## REFERENCES

Bailey, S. C. C., Hultmark, M., Schumacher, J., Yakhot, V. & Smits, A. J. 2009 Measurement of local dissipation scales in turbulent pipe flow. *Phys. Rev. Lett.* **103**, 014502.

Boeck, T., Krasnov, D. & Schumacher, J. 2010 Statistics of velocity gradients in wall-bounded shear flow turbulence. *Physica* D (in press) (doi:10.1016/j.physd.2009.10.004).

Durst, F., Jovanovic, J. & Sender, J. 1995 LDA measurements in the near-wall region of a turbulent pipe flow. *J. Fluid Mech.* **295**, 305–335.

Frisch, U. 1995 *Turbulence: The Legacy of A. N. Kolmogorov*. Cambridge University Press.

Gioia, G. & P. Chakraborty, P. 2006 Turbulent friction in rough pipes and energy spectrum of phenomenological theory. *Phys. Rev. Lett.* **96**, 044502.

Hoyas, S. and Jimenez, J. 2005 Scaling the velocity fluctuations in turbulent channels up to $Re_\tau = 2003$. In *Annual Research Briefs 2005*, Center for Turbulence Research, 351–356.

Hoyas, S. & Jiménez, J. 2006 Scaling of the velocity fluctuations in turbulent channels up to $Re_\tau = 2003$. *Phys. Fluids* **18**, 011702.

Hultmark, M., Bailey, S. C. C. & Smits, A. J. 2010 Scaling of near-wall turbulence in pipe flow. *J. Fluid Mech.* **649**, 103–113.

Hutchins, N., Nickels, T. B. Marusic, I. & Chong, M. S. 2009 Hot-wire spatial resolution issues in wall-bounded turbulence. *J. Fluid Mech.* **635**, 103–136.

Kim, J., Moin, P. & Moser, R. 1987 Turbulence statistics in fully developed channel flow at low Reynolds number. *J. Fluid Mech.* **177**, 133–166.

Lee, C., Yeo, K. & J. Choi 2004 Intermittent nature of acceleration in near wall turbulence. *Phys. Rev. Lett.* **92**, 144502.

Morrison, J. F., McKeon, B. J., Jiang, W. & Smits, A. J. 2004 Scaling of the streamwise velocity components in turbulent pipe flow. *J. Fluid Mech.* **508**, 99–131.

Nagib, H. M., Chauhan, K. A. & Monkiewitz, P. A. 2007 Asymptotic state for zero pressure gradient turbulent boundary layers. *Phil Trans. R. Soc.* A **365**, 755–770.

Schlichting, H. 1968 *Boundary-Layer Theory*. McGraw-Hill.

Schumacher, J. 2007 Sub-Kolmogorov-scale fluctuations in fluid turbulence. *Europhys. Lett.* **80**, 54001-1–54001-6.

Schumacher, J., Sreenivasan, K. R. & Yakhot, V. 2007 Asymptotic exponents from low-Reynolds-number flows. *New. J. Phys.* **9**, 89 (doi:10.1088/1367-2630/9/4/089).

Wu, X. & Moin, P. 2008 A direct numerical simulation study on the mean velocity characteristics in turbulent pipe flow. *J. Fluid Mech.* **608**, 81–112.

Yakhot, V. 2006 Probability densities in strong turbulence. *Physica* D **215**, 166–174.

Zagarola, M. V. & Smits, A. J. 1998 Mean flow scaling of turbulent pipe flow. *J. Fluid Mech.* **373**, 33–79.

Zhao, R. & Smits, A. J. 2007 Wall-normal turbulence statistics in high Reynolds number pipe flow. *J. Fluid Mech.* **576**, 457–473.